

## Diffusion, Dispersion, and Settling of Hard Spheres

J.-Z. Xue,<sup>(1),(2)</sup> E. Herbolzheimer,<sup>(1)</sup> M. A. Rutgers,<sup>(2)</sup> W. B. Russel,<sup>(3)</sup> and P. M. Chaikin<sup>(1),(2)</sup>

<sup>(1)</sup>*Exxon Research and Engineering Company, Route 22 East, Annandale, New Jersey 08801*

<sup>(2)</sup>*Department of Physics, Princeton University, Princeton, New Jersey 08540*

<sup>(3)</sup>*Department of Chemical Engineering, Princeton University, Princeton, New Jersey 08540*

(Received 19 May 1992)

Using a multiple light scattering technique and a stabilizing counterflow (i.e., a fluidized bed), we measured the average sedimentation velocity, its variance, and the short-time self-diffusion coefficient in a concentrated hard-sphere suspension. Many-body hydrodynamic interactions slow both the Brownian diffusion and mean sedimentation and provide a novel mechanism for long time dispersion.

PACS numbers: 82.70.Dd, 05.40.+j, 66.20.+d, 66.90.+r

When the particles in a suspension are denser than the suspending solvent, their motions are controlled by sedimentation as well as the customary diffusion due to stochastic thermal fluctuations. As the particle concentration is increased, many-body hydrodynamic interactions strongly modify the settling and diffusion. Both of these processes are fundamental to a variety of natural and industrial systems. They also represent some of the most difficult problems in statistical physics and hydrodynamics.

In a concentrated hard-sphere colloidal suspension, Brownian motion is altered not only by direct potential interactions, but also by solvent mediated many-body hydrodynamic interactions [1-6]. The motion of any particle creates a disturbance flow in the surrounding solvent which diffuses with a characteristic viscous time  $\tau_v = R^2\rho/\eta$  with  $R$  being the radius of the particle,  $\rho$  the density of the solvent, and  $\eta$  the viscosity of the solvent. On time scales less than or comparable to  $\tau_v$ , the particle motion is non-Brownian due to the transient development of the flow field. At times sufficiently longer than  $\tau_v$ , the particles execute Brownian motion hindered by the increased flow resistance due to neighboring particles.

Superposed on this Brownian motion is the sedimentation due to gravity. Here the hydrodynamic interactions play a key role in determining the drag and hence the settling velocity of each particle. A single sphere in a solvent settles at the well-known Stokes velocity  $V_0 = \frac{2}{9} R^2(\rho' - \rho)g/\eta$ , where  $\rho'$  is the density of the sphere. In a uniform concentrated suspension, the settling of the particles induces a compensating backflow of solvent which reduces the average sedimentation velocity because the solvent has to flow through narrower channels controlled by the interparticle spacing. At the same time, each particle settles with a different velocity determined by the particular configuration of its neighbors. For example, two particles close together experience the downward flow created by the other and, hence, both settle faster than if spatially separated. In addition, the pair will drift horizontally if not oriented either horizontally or vertically. Thus a given particle settles at roughly the same speed until the configuration of its neighbors is significantly changed. Recent computer simulations [7,8]

and direct observations at low volume fraction in quiescent sedimentation experiments [9] show that the particles settle on the order of 100 interparticle distances before assuming a different speed. Therefore, in a concentrated colloidal suspension particles settle with a distribution of velocities, both vertically and horizontally, which on long time scales causes the particles to drift apart randomly at a rate much larger than that due to Brownian motion. The calculation and measurement of the average sedimentation velocity and its variance as a function of volume fraction for the hard-sphere suspension is a fundamental test of our understanding of hydrodynamic interactions.

In this Letter, we report our measurements on the hindered mean sedimentation velocity and its variance for concentrated hard-sphere colloidal suspensions. By employing a fluidized bed, in which the solvent is flowing upward to counterbalance the sedimentation, we obtain a uniform colloidal suspension that is distinguished from other systems in that any transient disturbances due to sample preparations are completely damped out and the volume fraction of the system is conveniently varied by changing the solvent flow rate. We have measured the average sedimentation velocity as a function of the particle volume fraction unambiguously. By using a multiple light scattering technique, we probe the motion of particles suspended in the fluidized bed and, therefore, directly measure the variance of sedimentation velocity at short times.

Our sample cell is made out of a rectangular glass tube. A Vycor filter paper with a pore size of 20 nm distributes the inlet flow uniformly across the sample cell. The suspension is contained in the straight portion of the cell with cross section 2 mm  $\times$  20 mm. The colloidal particles are polystyrene spheres  $15.5 \pm 0.2 \mu\text{m}$  in diameter purchased commercially. In distilled water, these particles can be approximated as hard spheres. In our experiments, we first put a known amount of the polystyrene spheres in the fluidized bed. Water from the reservoir flows through the filter (distributor) and uniformly upward in the straight portion of the sample cell, fluidizing the suspension. The concentration in the suspended colloidal column is very uniform, as indicated by laser

transmission and particle dynamics measurements at several vertical positions. The particle Reynolds number,  $2RV_0\rho/\eta \sim 10^{-4}$ , is low, indicating that the solvent undergoes creeping flow, i.e., that inertial effects are negligible.

To measure the average sedimentation velocity as a function of the volume fraction, we only need to change the height of the solvent reservoir, hence the flow rate of the solvent, and after the steady state is reestablished measure the height of the suspended column to determine the volume fraction. Our results are plotted in Fig. 1. We also plot data for the sedimentation velocity from Ref. [10], which are in good agreement with ours.

Although the upward flow of the solvent counters the mean settling velocity, the particles still move due to thermal fluctuations and the variance in the settling velocities caused by hydrodynamic interactions between the particles. The thermal fluctuations lead to hindered Brownian motion [1-6,11,12]. On the other hand, on length scales less than the interparticle spacing, the variance in the settling velocity of an individual particle implies a motion with constant speed (different from the mean) and this leads to a relative displacement linear in time.

We measure this relative displacement of the particles using dynamic light scattering. Although the polystyrene spheres in our experiments are fairly large, they still strongly scatter light, and a typical fluidized colloidal suspension in our experiments looks white and opaque. This, in part, prevents us from studying the particle dynamics using conventional single light scattering techniques. However, we can employ diffusing wave spectroscopy (DWS), the dynamic light scattering technique in the strong scattering limit [13]. In DWS, appropriate analysis of the temporal fluctuations of multiply scattered light yields the particle dynamics. We employ the DWS technique in transmission mode in a similar manner as described previously [4,5]. A laser beam ( $\lambda_0=488$  nm) was expanded and collimated to uniformly illuminate a 1-cm-diam spot on one side of the fluidized bed containing the uniformly suspended particles. Light emerging

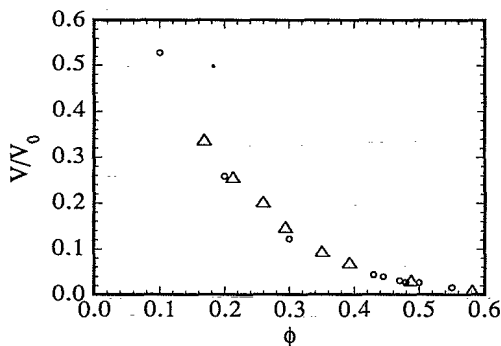


FIG. 1.  $\Delta$ , measured sedimentation velocity as a function of volume fraction.  $\circ$ , data from Ref. [10].

from the other side of the fluidized bed was detected by a photomultiplier, and the static intensity and temporal correlation function were measured using a correlator. By carefully choosing the sample thickness, we ensure multiple scattering and study the particle motion on a length scale that is a fraction of the interparticle spacing [13].

The detailed algorithm for DWS in transmission with broad illumination has been worked out many times and the electric field-field correlation function is given as [4,5]

$$g_1(t) = \frac{(L/l^* + \frac{4}{3})\sqrt{x}}{(1 + \frac{4}{9}x)\sinh(L\sqrt{x}/l^*) + \frac{4}{3}\sqrt{x}\cosh(L\sqrt{x}/l^*)}, \quad (1)$$

where  $L$  is the thickness of the sample,  $l^*$  is the transport mean free path of the photons, and  $x = k_0^2 \langle \Delta r^2(t) \rangle / [S(q)]$  with  $k_0$  being the wave vector,  $\langle \Delta r^2(t) \rangle$  the ensemble averaged particle displacements, and  $[S(q)]$  a  $q^3$ -weighted average of the structure factor  $S(q)$  of the colloidal suspension.

To calculate particle motion as a function of time from the measured electric field-field correlation function, we need to know  $[S(q)]$  and  $l^*$ . Computer simulations show that, although there is a small change, the structure factor  $S(q)$  for a sedimenting suspension is close to that for a neutrally buoyant suspension at the same concentration [7]. For polystyrene spheres 15.5  $\mu\text{m}$  in diameter,  $[S(q)] \sim 1$  and we measure individual particle motions [5].

The transport mean free path  $l^*$ , in the case when  $[S(q)] \sim 1$ , is inversely proportional to the volume fraction  $\phi$  and can be extracted from the absolute transmitted intensity [14]. In our experiments, we compare the transmission with that of a standard cell, a suspension of uniform polystyrene spheres (diameter of 0.412  $\mu\text{m}$ ) at  $\phi = 0.0087$  in the same container to properly account for reflections due to sample boundaries [15]. The transport mean free path for the standard cell can be measured with DWS, and, by comparison, we obtain  $l^*$  for the fluidized suspension [5]. We find that  $L/l^*$  for our sample ranges from 6.3 to 16.8 from the lowest to the highest  $\phi$  in our experiments.

With the knowledge of  $l^*$  and  $[S(q)]$ , we can invert the measured  $g_1(t)$  to obtain particle displacements as a function of time. To analyze the measured  $\langle \Delta r^2(t) \rangle$ , we note that the characteristic time  $\tau_v \sim 61.3$   $\mu\text{s}$ , which is comparable to the time range over which the measured  $g_1(t)$  decays significantly. The particle motion due to stochastic thermal fluctuations is therefore not simply diffusive [11] and the Langevin equation must be used. Because of the linearity of the Langevin equation, we can separate the contributions to  $\langle \Delta r^2(t) \rangle$  as follows:

$$\langle \Delta r^2(t) \rangle = \langle \Delta r^2 \rangle_v + 6 \langle \Delta V \rangle^2 t^2, \quad (2)$$

where  $\langle \Delta V \rangle$  is an average of the variance in the sedimentation

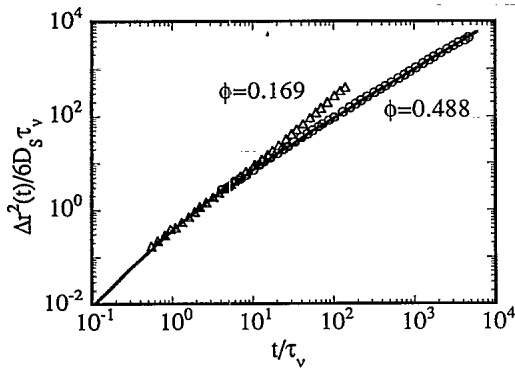


FIG. 2. Particle displacement  $\langle \Delta r^2 \rangle$  as a function of time for two volume fractions. The symbols are experimental data and the solid line is the analytical solution calculated by Hinch in a single-particle limit [11]. The time is scaled by  $\tau_v$  and the displacement by  $6D_s \tau_v$ .

tation velocity [16] that results from convective motion and contributes to  $\langle \Delta r^2(t) \rangle$  quadratically in time at very short time and length scales. The first term in Eq. (2),  $\langle \Delta r^2 \rangle_v$ , represents the mean-square displacements due to the stochastic non-Brownian motion. In the single-particle limit, Hinch obtained an analytical solution for  $\langle \Delta r^2 \rangle_v$  [11]. In a concentrated suspension, Zhu *et al.* have recently shown that  $\langle \Delta r^2 \rangle_v$  exhibits the same form except that the single-particle Stokes diffusion coefficient,  $D_0 = kT/6\pi\eta R$ , and the viscous time,  $\tau_v^0 \equiv \tau_v(\phi=0)$ , are replaced by concentration-dependent short-time self-diffusion coefficient  $D_s$  and viscous relaxation time  $\tau_v$  [12]. Furthermore, in the concentration range they studied, Zhu *et al.* found that  $\tau_v$  is given by  $R^2\rho/\eta(\phi)$ , where  $\eta(\phi)$  is the high-frequency, low-strain viscosity of the suspension [12,17,18].

In Fig. 2 we show the measured mean-square displacements  $\langle \Delta r^2 \rangle$  at volume fractions  $\phi = 0.169$  and  $0.488$ . It is noticeable that at the lower volume fraction  $\langle \Delta r^2 \rangle$  significantly deviates from the motion due to thermal fluctuations, indicating the importance of the contributions due to the variance in settling velocities. We fitted our measured  $\langle \Delta r^2 \rangle$  by Eq. (2) by adjusting  $D_s$ ,  $\tau_v$ , and  $\langle \Delta V \rangle$ . In Fig. 3 we plot the values we obtained for  $D_s/D_0$  and  $\tau_v/\tau_v^0$  as well as  $\tau_v/\tau_v^0$  obtained by Zhu *et al.* [12]. Our experimentally determined  $D_s$  agrees well with both theoretical (low concentration) and experimental values of the short-time self-diffusion coefficients reported in the literature [1,4,5,19].

In Fig. 4 we plot our values of the variance in the sedimentation velocity normalized by the Stokes velocity and its value normalized by the mean settling velocity at the given  $\phi$ . The variance is comparable to the mean sedimentation velocity at lower volume fractions, but as  $\phi$  increases,  $\langle \Delta V \rangle$  decreases faster than the mean. This presumably reflects the fact that the crowded configurations at higher concentrations look more alike throughout the sample.

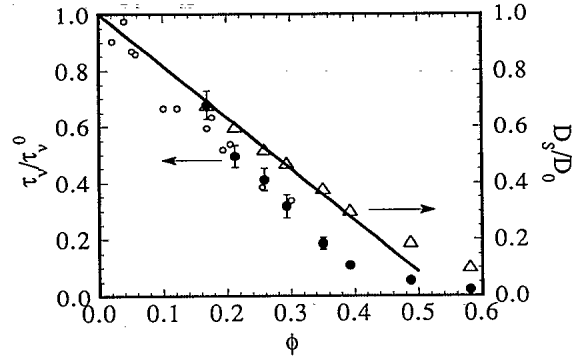


FIG. 3.  $\Delta$ , measured  $D_s/D_0$  as a function of volume fraction, where  $D_0$  is the free diffusion coefficient. Solid line,  $D_s/D_0 = 1 - 1.83\phi$ .  $\bullet$ , measured  $\tau_v/\tau_v^0$  as a function of volume fraction in this experiment.  $\circ$ , data taken from Ref. [12].

Shear flow also contributes a convective ( $t^2$ ) term to  $\langle \Delta r^2(t) \rangle$  which might interfere with our interpretation of the variance [20]. However, for our maximum flow rate of  $3 \mu\text{m}/\text{sec}$  and the sample geometry any such contribution is orders of magnitude below the  $t^2$  term we measure from the variance.

In conclusion, we have studied particle dynamics in a uniform hard-sphere fluidized suspension. The fluidization provides a convenient way to control the particle concentration and allows transient effects to dissipate so that steady state measurements can be made. We have measured the effects of hydrodynamic interactions on the average sedimentation velocity and its variance, and the thermally driven diffusive processes. The sedimentation velocity variance is comparable to the mean but decreases quickly as volume fraction is increased. The particle motion which results from this variance is convective on a short time scale but is diffusive or dispersive on a time scale of several velocity changes or a distance scale of many interparticle spacings. For our samples at  $\phi \sim 0.2$  this dispersion is  $10^3$  larger than thermal diffusion.

We would like to thank D. J. Pine for his generous loan of equipment and useful discussions. We would also like

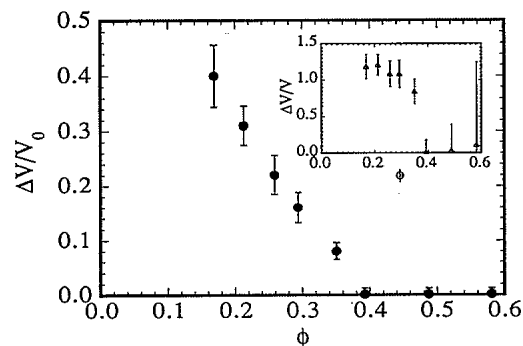


FIG. 4.  $\bullet$ , variance to the sedimentation velocity as a function of volume fraction. The bars are the error in the measurements. Inset: The ratio of the variance to the mean sedimentation velocity.

to thank D. A. Weitz for many helpful suggestions, especially regarding how to analyze the data at early times. This work was partially supported by the National Aeronautics and Space Administration.

- 
- [1] G. K. Batchelor, *J. Fluid Mech.* **74**, 1 (1976); **131**, 155 (1983).
- [2] C. W. J. Beenakker and P. Mazur, *Physica (Amsterdam)* **120A**, 388 (1983); **126A**, 349 (1984).
- [3] I. Snook, W. van Megan, and R. J. A. Tough, *J. Chem. Phys.* **78**, 5825 (1983).
- [4] X. Qiu, X. L. Wu, J. Z. Xue, D. J. Pine, D. A. Weitz, and P. M. Chaikin, *Phys. Rev. Lett.* **65**, 516 (1990).
- [5] J.-Z. Xue, X. L. Wu, D. J. Pine, and P. M. Chaikin, *Phys. Rev. A* **45**, 989 (1992).
- [6] S. Fraden and G. Maret, *Phys. Rev. Lett.* **65**, 512 (1990).
- [7] A. Ladd (to be published).
- [8] H.-M. Chan, Ph.D thesis, California Institute of Technology, 1988 (unpublished).
- [9] J. M. Ham and G. M. Homsy, *Int. J. Multiphase Flow* **14**, 533 (1988).
- [10] S. E. Paulin and B. J. Ackerson, *Phys. Rev. Lett.* **64**, 2663 (1990).
- [11] E. J. Hinch, *J. Fluid Mech.* **72**, 499 (1975).
- [12] J. X. Zhu, D. J. Durian, J. Müller, D. A. Weitz, and D. J. Pine, *Phys. Rev. Lett.* **68**, 2559 (1992).
- [13] D. J. Pine, D. A. Weitz, P. M. Chaikin, and E. Herbolzheimer, *Phys. Rev. Lett.* **60**, 1134 (1988).
- [14] A. Ishimaru, *Wave Propagation and Scattering in Random Media* (Academic, New York, 1978).
- [15] J. X. Zhu, D. J. Pine, and D. A. Weitz, *Phys. Rev. A* **44**, 3948 (1991).
- [16] J.-Z. Xue and P. M. Chaikin (to be published).
- [17] J. C. van der Werff, C. G. de Kruif, C. Blom, and J. Mellema, *Phys. Rev. A* **39**, 795 (1989).
- [18] R. J. Phillips, J. F. Brady, and G. Bossis, *Phys. Fluids* **31**, 3462 (1988).
- [19] W. van Megan, S. M. Underwood, R. H. Ottewill, N. St. J. Williams, and P. N. Pusey, *Faraday Discuss. Chem. Soc.* **83**, 47 (1987).
- [20] X. L. Wu, D. J. Pine, P. M. Chaikin, J. S. Huang, and D. A. Weitz, *J. Opt. Soc. Am. B* **7**, 15 (1990).